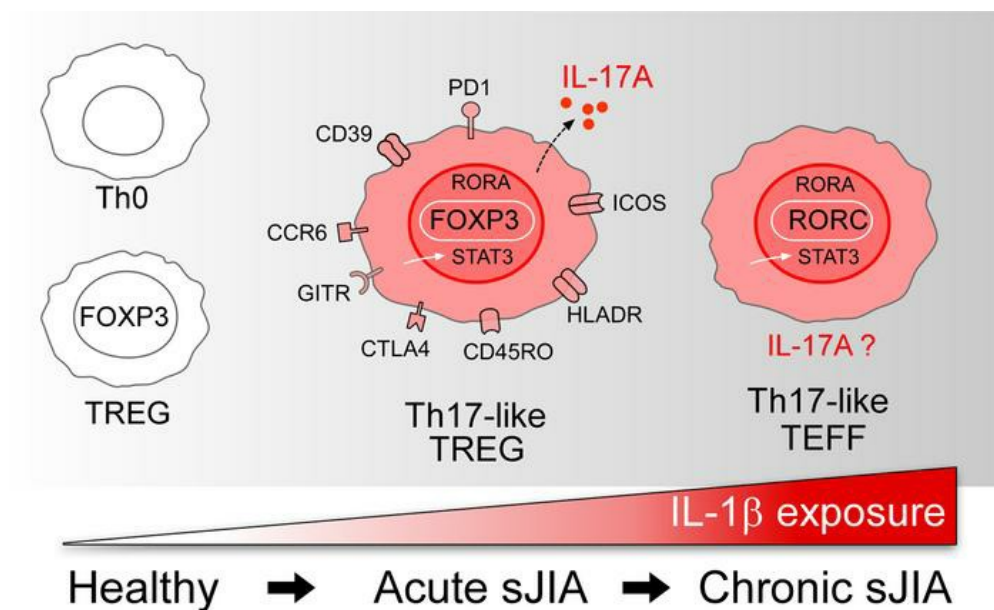# Th17 reprogramming of T cells in systemic juvenile idiopathic arthritis

Lauren A. Henderson, … , Talal A. Chatila, Peter A. Nigrovic

Research Article   Inflammation

## Graphical abstract

# Th17 reprogramming of T cells in systemic juvenile idiopathic arthritis

Lauren A. Henderson,[1] Kacie J. Hoyt,[1] Pui Y. Lee,[1,2] Deepak A. Rao,[2] A. Helena Jonsson,[2] Jennifer P. Nguyen,[3] Kayleigh Rutherford,[4] Amélie M. Julé,[1] Louis-Marie Charbonnier,[1] Siobhan Case,[1] Margaret H. Chang,[1,2] Ezra M. Cohen,[1] Fatma Dedeoglu,[1] Robert C. Fuhlbrigge,[1,5] Olha Halyabar,[1] Melissa M. Hazen,[1] Erin Janssen,[1] Susan Kim,[1] Jeffrey Lo,[1] Mindy S. Lo,[1] Esra Meidan,[1] Mary Beth F. Son,[1] Robert P. Sundel,[1] Matthew L. Stoll,[6] Chad Nusbaum,[7] James A. Lederer,[3] Talal A. Chatila,[1] and Peter A. Nigrovic[1,2]

[1]Division of Immunology, Department of Pediatrics, Boston Children's Hospital, Harvard Medical School, Boston, Massachusetts, USA. [2]Division of Rheumatology, Inflammation, and Immunity, Department of Medicine, and [3]Department of Surgery, Brigham and Women's Hospital, Boston, Massachusetts, USA. [4]Harvard Bioinformatics Core, Harvard School of Public Health, Boston, Massachusetts, USA. [5]Department of Rheumatology, Children's Hospital Colorado, Aurora, Colorado, USA. [6]Division of Pediatric Rheumatology, Department of Pediatrics, School of Medicine, University of Alabama at Birmingham, Birmingham, Alabama, USA. [7]Broad Technology Labs, Broad Institute, Massachusetts Institute of Technology and Harvard University, Cambridge, Massachusetts, USA.

Systemic juvenile idiopathic arthritis (sJIA) begins with fever, rash, and high-grade systemic inflammation but commonly progresses to a persistent afebrile arthritis. The basis for this transition is unknown. To evaluate a role for lymphocyte polarization, we characterized T cells from patients with acute and chronic sJIA using flow cytometry, mass cytometry, and RNA sequencing. Acute and chronic sJIA each featured an expanded population of activated Tregs uncommon in healthy controls or in children with nonsystemic JIA. In acute sJIA, Tregs expressed IL-17A and a gene expression signature reflecting Th17 polarization. In chronic sJIA, the Th17 transcriptional signature was identified in T effector cells (Teffs), although expression of IL-17A at the protein level remained rare. Th17 polarization was abrogated in patients responding to IL-1 blockade. These findings identify evolving Th17 polarization in sJIA that begins in Tregs and progresses to Teffs, likely reflecting the impact of the cytokine milieu and consistent with a biphasic model of disease pathogenesis. The results support T cells as a potential treatment target in sJIA.

## Introduction

Systemic juvenile idiopathic arthritis (sJIA) is distinguished from other forms of childhood arthritis through its distinctive presentation (1, 2). Disease onset is marked by fevers, rash, and markedly elevated inflammatory markers, often preceding the onset of arthritis by weeks or months (3). While sometimes self-limited, sJIA frequently transitions into a chronic inflammatory arthritis that can be resistant to treatment and cause substantial morbidity (4–7).

The pathogeneses of sJIA and its adult counterpart, adult-onset Still's disease (AOSD), remain poorly understood (8). Systemic JIA is sometimes categorized as an autoinflammatory disease by virtue of its intensely inflammatory acute presentation, balanced sex distribution, and lack of autoantibodies (9). Correspondingly, research in sJIA has focused primarily on innate immunity, including abnormalities in monocytes, neutrophils, NK cells, myeloid-derived S100 proteins, and IL-18 signal transduction (10–16). The success of treatment directed against IL-1, IL-6, and — more recently — IL-18 further support this approach (17–20). However, it remains unclear why the disease evolves in some patients from an acute febrile phase to the devastating arthritis that often characterizes chronic sJIA.

The biphasic hypothesis postulates that the cytokine-rich environment of early sJIA engenders a population of pathogenic T cells that perpetuates arthritis, even independently of the original cytokine drive (21). This hypothesis arose out of the observation that first-line treatment of sJIA with the recombinant IL-1 receptor antagonist (rIL-1RA) anakinra was associated with rapid and complete arrest of disease in many

patients, whereas treatment of established arthritis was often less successful (22–24). This observation has proven robust (25, 26). Furthermore, a genome-wide association study identified a haplotype containing the HLA class II allele DR-B1*11 as the strongest carrier of sJIA risk, suggesting a role for antigen-driven CD4^{+} T cells (27, 28).

How sJIA-associated cytokines might drive the development of pathogenic T cells remains undefined. Undifferentiated CD4^{+} T cells exposed to IL-1β and/or IL-6 in the presence of TGF-β develop into Th17 cells, while — in the absence of IL-1β and IL-6 — these cells become Tregs (29–36). Differentiated Tregs remain plastic; exposure to IL-1β and IL-6 promotes IL-17 production while reducing expression of the canonical Treg transcription factor (TF) FOXP3 (33, 34, 36). Murine studies confirm that such lymphocyte skewing can cause joint inflammation. Arthritis arising through deletion of the gene encoding endogenous IL-1RA is mediated by T cells, both CD4 Th cells and IL-17–producing γδ T cells (37–39). In collagen-induced arthritis, IL-6 converts protective Tregs into pathogenic Th17 cells or "exTregs" (40, 41). Correspondingly, in humans, Th17 cells contribute to some types of arthritis, whereas Tregs can constrain inflammation (42–48).

Here, we test the biphasic hypothesis by characterizing T cells in acute and chronic sJIA. In new-onset sJIA, we show that some Tregs are subverted to a Th17 phenotype, whereas in established sJIA arthritis, CD4^{+} T effector cells (Teffs) express a Th17 gene signature, though rarely IL-17A itself. Th17 polarization is abrogated by early IL-1 blockade. These findings are consistent with a role for adaptive immunity in sJIA and may help to explain how early manipulation of the cytokine milieu averts the development of chronic arthritis.

## Results

*Patients.* To study the evolution of the immune response in sJIA, we evaluated patients with new-onset febrile sJIA (acute sJIA, *n* = 17) and longstanding chronic arthritis associated with sJIA (chronic sJIA, *n* = 15) (Table 1). Healthy adults, healthy children, and patients with nonsystemic forms of JIA with active arthritis were studied as controls. As expected, acute sJIA patients were young (mean age 5.7 years, SD ± 5.0 years), had a short duration of disease (mean 0.2 years, SD ± 0.1 years), and had markedly elevated inflammatory markers (mean erythrocyte sedimentation rate (ESR) 80 mm/hr, C-reactive protein (CRP) 6.0 mg/dL). Every effort was made to obtain blood samples from acute sJIA patients before medications were started; however, this was not always feasible. In the 7 acute sJIA patients who provided a blood sample while on immunomodulatory medications, duration of treatment was brief (Table 2). By contrast, chronic sJIA patients were older (mean age 17.8 years, SD ± 7.1 years) had longer disease duration (mean 11.5 years, SD ± 6.6 years) and had received a range of immunosuppressive therapies (Table 1).

*A distinct population of Tregs resides in the arthritic joints of sJIA patients.* Two chronic sJIA patients provided paired blood and synovial fluid (SF) samples. To maximize the information gained from these rare samples, we employed mass cytometry to immunophenotype T cells using surface and intracellular markers (Supplemental Table 1; supplemental material available online with this article; https://doi.org/10.1172/jci.insight.132508DS1). Clusters of cells sharing cytometric properties were visualized using t-Distributed Stochastic Neighbor Embedding (viSNE) dimensional reduction (49). In both samples, Tregs (CD4^{+}CD25^{+}CD127^{lo}) exhibited conspicuously greater abundance in SF than in blood (Figure 1A). Pooled viSNE analysis of blood and SF Tregs showed that they segregated differently by surface markers (Figure 1B). In an individual patient, FOXP3 expression was similar in Tregs from the blood and SF (Figure 1C). Compared with blood Tregs, sJIA SF Tregs exhibited enhanced expression of memory, activation, and proliferation markers (CD45RO, HLADR, PD1, ICOS, Ki67), as well as Treg-related TFs and effector molecules (HELIOS, CTLA4, GITR, CD39) (Figure 1C). CCR6 and CD161, cell surface markers expressed on Th17 cells, were also upregulated (Figure 1C). Consistent with these findings, global transcriptomic analysis on sorted CD4^{+}CD25^{+}CD127^{lo} Tregs confirmed increased transcription of *PDCD1* (PD1), *ICOS*, *MKI67* (Ki67), *IKZF2* (HELIOS), *CTLA4*, *TNFRSF18* (GITR), *ENTPD1* (CD39), *CCR6*, and *KLRB1* (CD161) in SF Tregs compared with circulating Tregs from these patients and from healthy adult controls (*n* = 4) (Supplemental Figure 1).

*A subset of circulating sJIA Tregs phenotypically resembles SF Tregs.* While SF and blood Tregs were globally distinct, we evaluated whether a subpopulation of circulating Tregs resembled their SF counterparts. viSNE analysis was conducted on gated Tregs from acute sJIA blood (*n* = 6), chronic sJIA blood (*n* = 4), chronic sJIA SF (*n* = 2), and healthy control blood (*n* = 6). Samples were pooled by group to increase the ability to detect rare subpopulations. Indeed, a subset of Tregs from both acute and chronic sJIA blood

## Table 1. Patient Characteristics

| | Acute sJIA (n = 17) | Chronic sJIA (n = 15) | HC Pedi (n = 6) | HC Adult (n = 7) | JIA (n = 14) |
|---|---|---|---|---|---|
| Age, yrs (mean ± SD) | 5.7 ± 5.0 | 17.8 ± 7.1 | 8.9 ± 4.0 | 31.5 ± 4.5 | 7.4 ± 5.0 |
| Gender (% female) | 47 | 80 | 67 | 43 | 79 |
| Disease Duration, yrs (mean ± SD) | 0.2 ± 0.1 | 11.5 ± 6.6 | | | 2.4 ± 3.0 |
| Current MAS (# patients) | 4 | 2 | | | |
| Joint Count (mean ± SD) | 3 ± 2.3 | 3 ± 3.9 | | | 2 ± 1.1 |
| ESR, mm/hr (mean ± SD) | 80 ± 35.8 | 18 ± 20.7 | | | 14 ± 8.1 |
| CRP, mg/dl (mean ± SD) | 6.0 ± 4.1 | 1.9 ± 3.3 | | | 0.8 ± 1.3 |
| Medications (# pts) | 2 | 7 | | | 2 |
|   Glucocorticoids | 0 | 8 | | | 4 |
|   DMARDs | 0 | 4 | | | 2 |
|   TNFα Inhibitor | 0 | 1 | | | 0 |
|   Abatacept | 6 | 1 | | | 0 |
|   Anakinra | 0 | 2 | | | 0 |
|   Canakinumab | 1 | 2 | | | 0 |
|   Tocilizumab | | | | | |

[A]A patient was considered as having MAS if he or she met the 2016 Classification Criteria for MAS Complicating sJIA at the time of the biosample collection (55). sJIA, systemic juvenile idiopathic arthritis; HC, healthy control; pedi, pediatric; JIA, juvenile idiopathic arthritis (non-systemic JIA); MAS, macrophage activation syndrome ESR, erythrocyte sedimentation rate; CRP, C-reactive protein; DMARDs, disease-modifying antirheumatic drugs. Medications refers to treatment at time of sampling.

localized by viSNE in close proximity to SF Tregs, indicating a shared cytometric phenotype (Figure 2, A–C). These Tregs were less frequent in the blood of healthy controls (Figure 2D). At the individual level, this population was identified in each of the acute sJIA (mean 15.4% of Tregs, SD ± 17.2%) and chronic sJIA (14.8% ± 12%) patients included in the concatenated analysis at a higher average frequency than controls (5.6% ± 2.5%), although the difference did not reach statistical significance (Supplemental Figure 2).

To further assess the viSNE findings, hierarchical clustering by Spanning-tree Progression Analysis of Density-normalized Events (SPADE) was performed on Tregs from the concatenated samples of acute sJIA blood (*n* = 6), chronic sJIA blood (*n* = 4), chronic sJIA SF (*n* = 2), and healthy control blood (*n* = 6). SPADE identified the same dominant population of SF Tregs as noted by viSNE (Figure 2E and Supplemental Figure 3). This subgroup of Tregs was found in the blood of both acute and chronic sJIA patients (15.2% and 16.2% of all Tregs, respectively), compared with 6.1% in controls (Figure 2, E–H). As with Tregs in sJIA SF, this subpopulation identified by both viSNE and SPADE expressed high levels of CD45RO, HLADR, ICOS, Ki67, HELIOS, CTLA4, and CD39 (Figure 2). PD1 and GITR were not expressed as highly in this subset of blood Tregs as in SF Tregs.

While CD4 memory T cells were also more abundant in SF than blood (Figure 1A), viSNE failed to identify marked cytometric differences between compartments (Supplemental Figure 4). Extending viSNE to this population, with Tregs gated out of the analysis, we could not identify a population of memory $CD4^+$ T cells in SF and blood from sJIA patients that was distinct from cells present in controls (Supplemental Figure 5). Thus, the most prominent abnormality in sJIA T cells, most strikingly in SF but also in blood, was an increased frequency of Tregs bearing markers of memory, activation, and proliferation.

*Tregs in acute sJIA patients express IL-17.* Flow cytometry was employed to further define the phenotype and cytokine expression of Tregs in sJIA. The frequency of Tregs ($CD4^+CD25^+FOXP3^+$) in the blood of patients with sJIA resembled the frequencing of Tregs in control adults and children, as well as in patients with other types of JIA (Supplemental Figure 6). HELIOS is a marker of Treg lineage stability and promotes Treg suppressive function; acute sJIA patients had the highest frequency of HELIOS[hi] Tregs, although this proportion differed significantly only between acute and chronic sJIA (Supplemental Figure 6, B and C) (50–54). The frequency of circulating $CTLA4^+$ Tregs was comparable across groups (Supplemental Figure 6, B and C).

Tregs in the blood of healthy controls and patients with active nonsystemic JIA rarely expressed IL-17A (Figure 3, A and B). By contrast, the frequency of circulating $IL-17A^+$ Tregs was increased in acute sJIA (mean ± SD, 4.8% ± 3.1%) compared with all other groups ($P \leq 0.0001$ by 1-way ANOVA with multiple comparisons) (Figure 3, A and B). In some acute sJIA patients, up to 10% of Tregs in blood were $IL-17A^+$

**Table 2. Medication use in acute sJIA patients**

| Patient | Age (yrs) | Sex | Joint count | ESR (mm/hr) | CRP (mg/dL) | Medication |
|---------|-----------|-----|-------------|-------------|-------------|------------|
| sJIA1 | 5.9 | F | 5 | 104 | 8.0 | Toci × 1 dose, Pred × 19 days |
| sJIA2 | 4.0 | F | 2 | 90 | 4.08 | Anakinra × 4 days |
| sJIA3 | 1.6 | M | 1 | 140 | 3.04 | Anakinra × 4 days |
| sJIA4 | 5.1 | F | 6 | 78 | 3.5 | Anakinra × 2 days |
| sJIA5 | 1.2 | M | 3 | 68 | 10.0 | Anakinra × 3 days |
| sJIA6 | 14.3 | F | 8 | 31 | 0.67 | Anakinra × 8 days |
| sJIA7 | 5.4 | M | 4 | 46 | 1.97 | Anakinra × 4 days, Pred × 9 days |

sJIA, systemic juvenile idiopathic arthritis; ESR, erythrocyte sedimentation rate; CRP, C-reactive protein; Toci, Tocilizumab; pred, prednisone.

(Figure 3, A and B). The increased frequency of IL-17A$^+$ Tregs in acute sJIA was especially remarkable compared with pediatric controls, who had the lowest levels of IL-17A$^+$ Tregs (0.3% ± 0.3%). In acute sJIA, the proportion of IL-17A$^+$ cells was greater among Tregs (4.8% ± 3.1%) than among non-Treg CD4$^+$ T cells (CD4$^+$CD25$^-$, Teffs, 1.4 ±1.6%), CD4$^+$ memory T (1.6% ± 1.5%), and γδ T cells (0.3% ± 0.8%) (Figure 3, A–E). Acute sJIA patients with macrophage activation syndrome (MAS), as defined by the 2016 MAS Classification Criteria (55), had an especially high proportion of IL-17A$^+$ Tregs, although acute sJIA patients without MAS still exhibited a significant elevation compared with healthy controls and patients with other types of JIA (Figure 3F). The chemokine receptor CCR6 is a marker of Th17-like Tregs (41, 56). Indeed, the frequency of CCR6$^+$ and IL-17A$^+$ Tregs was positivity correlated ($r_s$ = 0.84, $P$ = 0.007) in our study subjects (Figure 3G). In acute sJIA patients, all evaluated IL-17A$^+$ Tregs coexpressed CCR6 (Figure 3G and Supplemental Figure 7). Consistent with IL-17 expression data, a greater proportion of Tregs but not CD4$^+$ memory T cells expressed CCR6 in acute sJIA patients (mean ± SD, 26.8% ± 13.6%) than in pediatric controls (7.0% ± 1.0%) ($P$ = 0.02) (Figure 3H). By contrast, the frequency of IL-17A$^+$ Tregs in chronic sJIA patients was not significantly higher than controls, nor was the proportion of cells expressing IL-17A elevated in Teffs, CD4$^+$ memory T cells, and γδ T cells in either acute or chronic sJIA (Figure 3, B–E). IFN-γ expressing Tregs were numerically increased in acute and chronic sJIA patients compared with controls, but this did not reach statistical significance (Figure 3B). The frequency of IFN-γ$^+$ γδ T cells was lower in acute sJIA than in pediatric controls ($P \leq 0.01$) or nonsystemic JIA patients ($P \leq 0.05$) (Figure 3E). Thus, acute sJIA is characterized by enhanced IL-17A expression restricted to the Treg population.

*Cytokine-expressing Tregs in acute sJIA are genuine Tregs.* To ensure that the cytokine-expressing Tregs identified in acute sJIA are in fact Tregs, we evaluated suppressive capacity and DNA methylation. Tregs were sorted by cell surface markers (CD4$^+$CD25$^+$CD127$^{lo}$) to avoid permeabilization and cell death. The frequency of IL-17A$^+$ and IFN-γ$^+$ cells was similar in Tregs defined by cell surface markers (CD4$^+$CD25$^+$CD-127$^{lo}$) and intracellular FOXP3 (CD4$^+$CD25$^+$FOXP3$^+$), indicating that both gating strategies identified the same population of cells (Supplemental Figure 8). sJIA Tregs from blood and SF maintained their ability to suppress proliferation of Teffs from a common healthy third-party donor (Figure 4, A–C). Tregs from sJIA blood and SF displayed typical Treg-specific demethylation patterns in the conserved noncoding sequence 2 (CNS2) region of *FOXP3* (Figure 4, D and E). Thus, the enriched population of CD4$^+$CD25$^+$CD127$^{lo}$ cells with enhanced IL-17 expression in acute sJIA maintained phenotypic features of bona fide Tregs.

*Tregs from acute sJIA patients express a Th17 gene signature.* Global transcriptomic analysis was performed on sorted blood Tregs (CD4$^+$CD25$^+$CD127$^{lo}$) from acute sJIA patients ($n$ = 8) and compared with healthy pediatric controls ($n$ = 5). During quality control, 2 pediatric control samples were excluded because of low total and mapped reads. Sixteen genes were differentially expressed in circulating Tregs from acute sJIA patients compared with pediatric controls at an FDR of <0.05 (Supplemental Table 2). Gene set enrichment analysis (GSEA) identified increased expression of Th17-related TFs (normalized enrichment score 1.35, FDR < 0.08) (Figure 5, A and B). Several key Th17 lineage–related TFs, including *RUNX1, BATF, RORA*, and *STAT3*, were among the genes in the leading-edge subset that contributed most to this result (57–59). Consistent with the absence of enhanced IL-17 expression in CD4$^+$ Teffs, no comparable signature could be identified in CD3$^+$CD4$^+$CD25$^-$ cells sorted from the same acute sJIA patients (Supplemental Figure 9). Circulating Tregs from acute sJIA also exhibited upregulation in gene pathways involved in TNF-α signaling, MYC targets, MTORC1 signaling, apoptosis, the unfolded protein response,
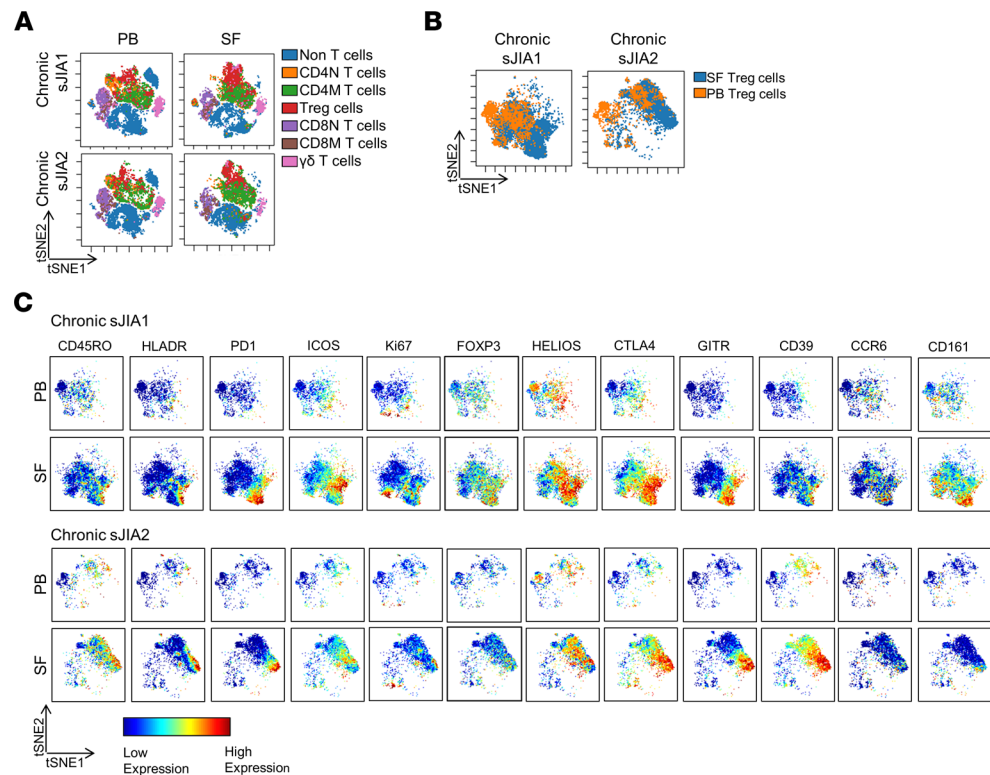
**Figure 1. A distinct population of Tregs is identified in the synovial fluid of sJIA patients with chronic arthritis. (A)** viSNE plots of mass cytometry of live, single cells from 2 chronic sJIA patients with paired peripheral blood (PB) and synovial fluid (SF) samples. The color indicates the lymphocyte populations, which were manually gated and overlaid onto the viSNE plots. (**B**) Gated, live, single Tregs (CD4+CD25+CD127lo) from the PB and SF of each chronic sJIA patient were analyzed together by viSNE and overlaid on the same viSNE plot. (**C**) viSNE plots of mass cytometry of PB and SF Tregs from 2 sJIA patients with paired PB and SF samples. The color indicates cell expression level of the labeled marker. viSNE analysis was performed with Cytobank. sJIA, systemic juvenile idiopathic arthritis; N, naive; M, memory; viSNE, visualization using t-Distributed Stochastic Neighbor Embedding; tSNE, t-Distributed Stochastic Neighbor Embedding.

the inflammatory response, complement, and oxidative phosphorylation (Figure 5A). The human Treg transcriptional signature sourced from ref. 60 was also evaluated in acute sJIA Tregs compared with pediatric controls, without substantial difference (normalized enrichment score 1.2, FDR = 0.58).

*Teffs in the blood and SF from sJIA patients with chronic arthritis upregulate Th17-related genes.* Gene expression was evaluated in sorted circulating Teffs (CD3+CD4+CD25−) from patients with chronic sJIA ($n = 7$) by RNA sequencing (RNA-seq). These 7 chronic sJIA patients had longstanding disease and were much older than the acute sJIA patients (average age, 19 years). Since cytokine-expressing T cells occur at higher frequencies in adults compared with children, we compared chronic sJIA with healthy adult controls ($n = 4$) (61). A total of 190 genes were differentially expressed in blood Teffs from chronic sJIA patients compared with controls at an FDR < 0.05 (Supplemental Table 3). GSEA identified elevated expression of the IL-6/JAK/STAT3 pathway (normalized enrichment score 1.60, FDR < 0.02) and Th17-related TFs (1.44, FDR < 0.06) in chronic sJIA blood Teffs compared with adult controls (Figure 5, C–E). In the IL-6/JAK/STAT3 gene set, *IL17RA* and *STAT3* were among the genes in the leading-edge subset. Lineage-defining Th17-related TFs including *IRF4*, *STAT3*, *RORA*, *BATF*, and *RORC* were in the leading edge of the Th17 TF gene set analysis (57, 58). TNF-α–, IFN-γ–, and IFN-α–related pathways were also upregulated in chronic sJIA blood Teffs (Figure 5C). Thus, despite our inability to demonstrate IL-17 expression in Teffs (CD4+CD25−) or CD4+CD45RO+ T cells in chronic sJIA (Figure 3, C and D), Teffs from this population still exhibited evidence of Th17 polarization.

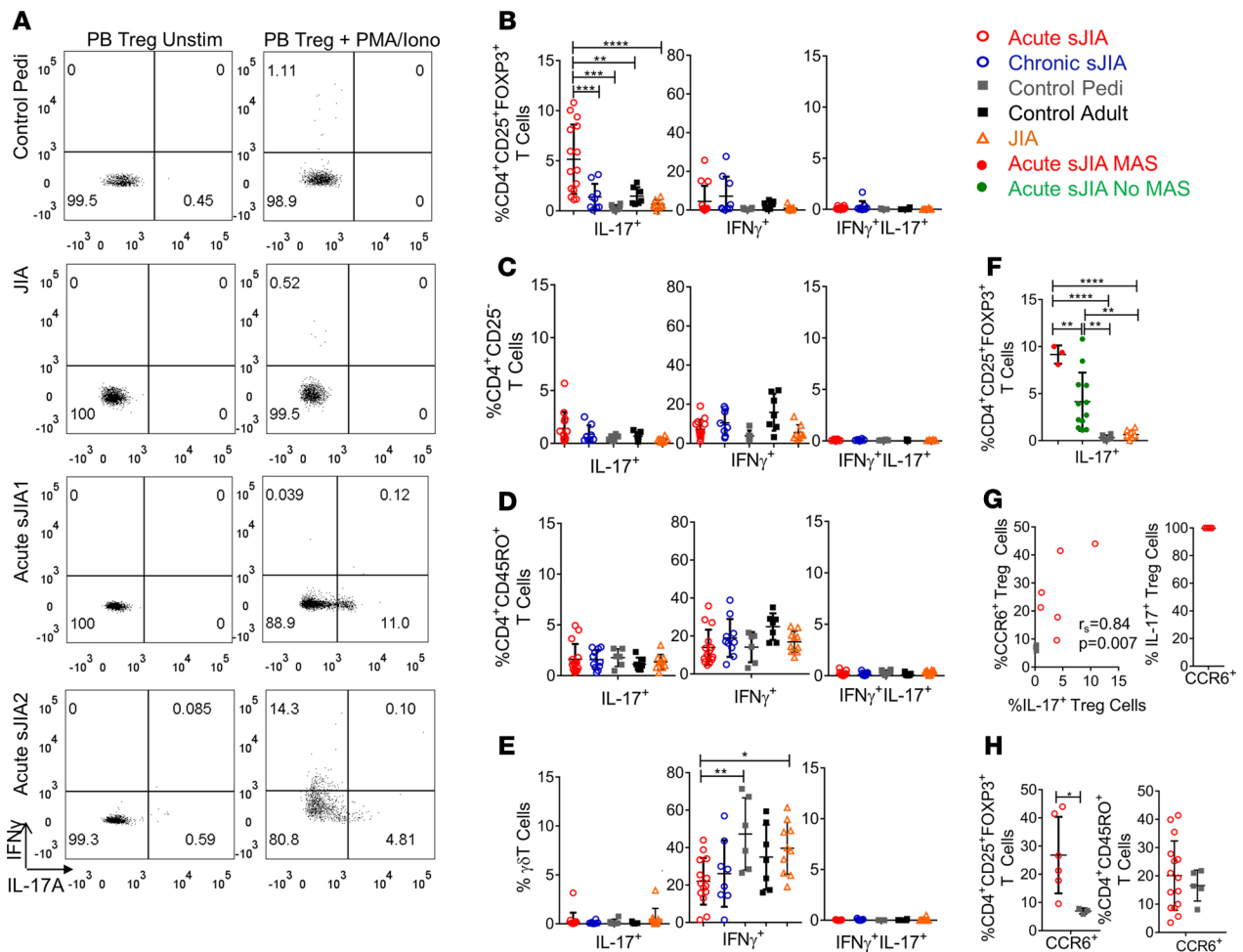Expression of Th17 pathway–related genes was similarly upregulated in Teffs from the arthritic joints of chronic sJIA patients compared with healthy control blood, including markers associated with pathogenic Th17 cells (*CSF2*, GM-CSF) (Figure 5F) (62, 63). In-depth analysis was limited, given the number of SF samples available ($n = 2$). Tregs from sJIA SF maintained expression of lineage-specific
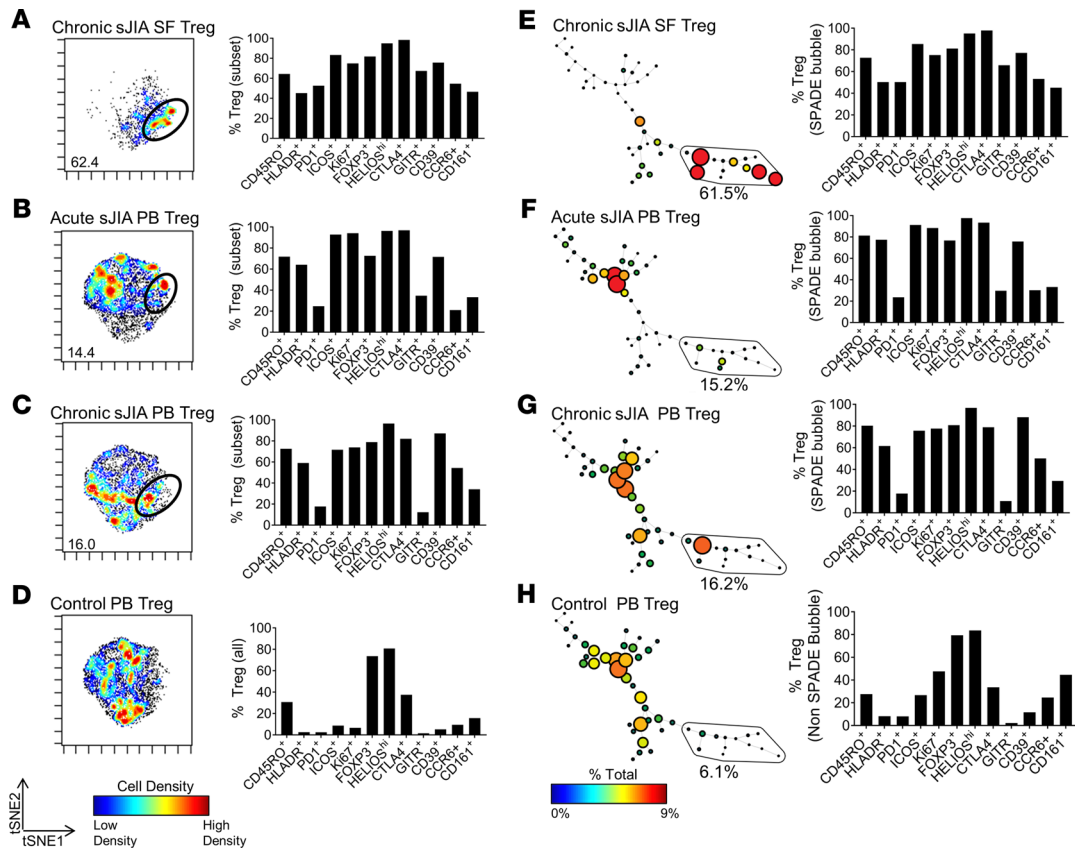
**Figure 2. A subpopulation of Tregs in the peripheral blood of sJIA patients share a mass cytometric phenotype with sJIA synovial fluid Tregs.** (**A–H**) Mass cytometry data of Tregs (CD4+CD25+CD127lo) were concatenated by study subject group, chronic sJIA SF (*n* = 2), acute sJIA PB (*n* = 6), chronic sJIA PB (*n* = 4), and controls (*n* = 6), and evaluated by viSNE and SPADE. (**A–D**) viSNE plots of mass cytometry of Tregs are depicted. The black circles on the viSNE plots in **B** and **C** highlight a population of Tregs that are cytometrically similar to SF Tregs depicted in **A** based on the location of the cells on the viSNE plot. The cell markers expressed in the population of Tregs identified on the viSNE plots by the black circle are shown in the accompanying bar graphs. (**D**) For healthy controls who lacked this population of Tregs, the expression of cell markers in all Tregs on the viSNE plot is depicted. (**E–H**) SPADE visualization of the same data. The size of the nodes reflects cell number, and the color of the node reflects the percent of total events. The bubbled nodes (black circle) on the SPADE trees captures the dominate population of Tregs in sJIA SF. The cell markers expressed on Tregs in the SPADE bubble are shown in the accompanying bar graphs. (**H**) For healthy controls who had a small number of cells in the SPADE bubble, the expression of cell markers on Tregs outside of this bubble are depicted. viSNE and SPADE analyses were performed with Cytobank. sJIA, systemic juvenile idiopathic arthritis; PB, peripheral blood; SF, synovial fluid; viSNE, visualization using t-Distributed Stochastic Neighbor Embedding; tSNE, t-Distributed Stochastic Neighbor Embedding; SPADE, spanning-tree progression analysis of density-normalized events.

TFs and effector molecules (Supplemental Figure 10A). Some Th17-related genes such as *RORA*, *CCR6*, *IL17RA,* and *CSF2* were upregulated in SF Tregs (Supplemental Figure 10B). Interestingly, sJIA SF Tregs expressed *IL1R1,* which has been previously shown to be expressed on Tregs that adopt a Th17 phenotype in response to IL-1 signaling (Supplemental Figure 10B) (64). Overall, the Th17 signature was not as robust in SF Tregs as in SF Teffs and did not exhibit a consistent increase in *RORC* or *STAT3* expression (Supplemental Figure 10B).

*Treatment with IL-1 blockade abrogates IL-17 expression by Tregs.* Patients with sJIA treated early in disease with IL-1 blockade often exhibit a brisk and frequently complete therapeutic response (22, 26). Accordingly, we tested IL-17A expression in Tregs from patients with new-onset active sJIA (*n* = 13) and in patients with recently diagnosed sJIA who had received anakinra within 4 weeks of diagnosis and entered remission as defined by modified Wallace criteria (*n* = 7) (65). Treated patients exhibited a significantly lower frequency of circulating IL-17A+ Tregs (Figure 6, A and B). These included 4 individuals who provided pre- and posttreatment peripheral blood samples. In these acute sJIA patients, therapy reduced the frequency of IL-17A+ Tregs to levels comparable with controls (Figure 6C). Thus, early and effective IL-1 blockade is associated with resolution of Th17 skewing among Tregs in sJIA.

**Figure 3. Acute sJIA Tregs express IL-17 to a greater degree than other T cell subsets.** (**A**) Representative flow cytometry dot plots gated on Tregs (CD4⁺CD25⁺FOXP3⁺). (**B–E**) The mean percentage ± SD of IL-17⁺, IFN-γ⁺, and IL-17⁺IFN-γ⁺ Tregs (CD4⁺CD25⁺FOXP3⁺) (**B**), Teffs (CD4⁺CD25⁻) (**C**), CD4⁺ memory T cells (**D**), and γδ T cells (**E**) in the peripheral blood (PB) of acute sJIA (n = 15), chronic sJIA (n = 9), pediatric control (n = 6), adult control (n = 7), and nonsystemic JIA (n = 10) study subjects as assessed by flow cytometry (1- way ANOVA corrected for multiple comparisons, *P ≤ 0.05, **P ≤ 0.01, ***P ≤ 0.001; ****P ≤ 0.0001). (**F**) The mean percentage ± SD of IL-17⁺ Tregs in the PB of acute sJIA patients with (n = 3) and without MAS (n = 12), along with pediatric controls (n = 6) and patients with nonsystemic JIA (n = 10) (1-way ANOVA corrected for multiple comparisons, **P ≤ 0.01; ****P ≤ 0.0001). (**G**) The correlation between the proportion of CCR6⁺ and IL-17A⁺ PB Tregs in acute sJIA patients (n = 6) and healthy controls (n = 3) measured by Spearman's correlation coefficient. The frequency of CCR6⁺ cells within IL-17⁺ Tregs in the PB of acute sJIA patients (n = 6) as assessed by flow cytometry. (**H**) The mean percentage +SD of CCR6⁺ Tregs (acute sJIA, n = 6; pediatric control, n = 3) and CD4⁺ memory T cells (acute sJIA, n = 15; pediatric control, n = 6) in the PB as assessed by flow cytometry (Mann Whitney U test, P = 0.02). Pedi, pediatric; JIA, juvenile idiopathic arthritis; sJIA, systemic juvenile idiopathic arthritis; unstim, unstimulated; MAS, macrophage activation syndrome.

## Discussion

Systemic JIA and AOSD are unique among the primary immune-mediated arthritides in presenting explosively with fever and rash, often well before joint disease begins. An understandable focus on innate immunity has left adaptive immune dysfunction relatively unexplored. We show here that acute sJIA is characterized by an expanded population of activated Tregs that express IL-17 and a prominent Th17 gene expression signature. In chronic arthritis, this signature shifts to CD4⁺ Teffs. Acquisition of the Th17 signature is abrogated by early IL-1 blockade, implicating the cytokine milieu in this progression. These observations underscore the potential limitations of conceptualizing sJIA as an autoinflammatory disease. Rather, consistent with the biphasic hypothesis, our findings suggest that adaptive immunity may also play an important part in sJIA, especially as it becomes chronic.

Our studies build upon the work of others. Omoyinmi and colleagues identified a small increase in the rare IL-17–expressing CD4⁺ T cells in the blood of active and inactive sJIA patients compared with pediatric controls (61). Kessel et al. documented a similar increase, albeit below the significance threshold,
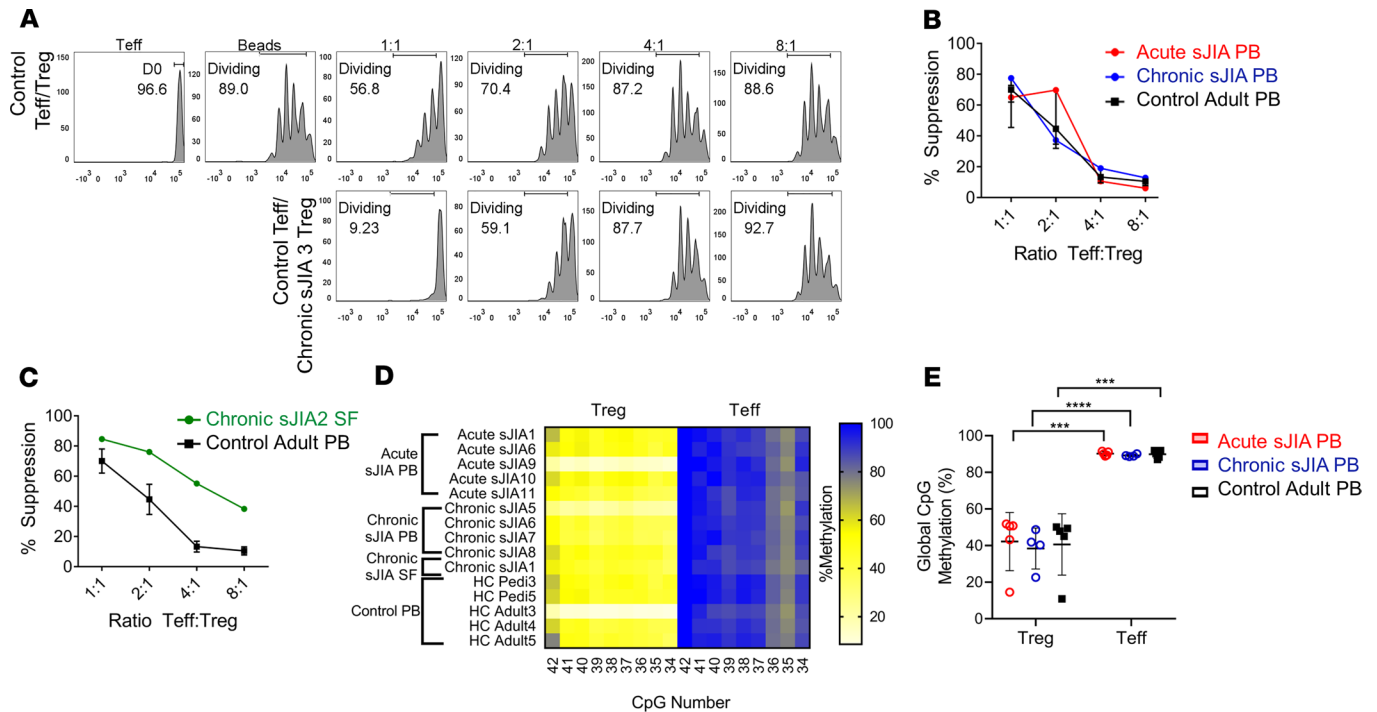
**Figure 4. Tregs in sJIA patients maintain suppressive capacity and CNS2 hypomethylation. (A)** Representative histograms from a healthy control and patient with chronic sJIA. CellTrace Violet–labeled peripheral blood (PB) Teffs from a third-party control were cultured alone, with autologous PB Tregs, or with sJIA PB Tregs at the given ratios after stimulation with anti-CD2/CD3/D28 beads. Teff proliferation was measured by flow cytometry as dye dilution. **(B)** The percent suppression of PB Teff proliferation from controls (*n* = 3) by autologous Tregs (CD4+CD25+CD127lo) at the given ratios (mean ± SEM). The percent suppression of PB Teff proliferation from a common third-party control by Tregs from acute sJIA (*n* = 3) and chronic sJIA (*n* = 4) are also depicted. **(C)** The percent suppression of PB Teff proliferation from controls (*n* = 3) by autologous Tregs (CD4+CD25+CD127lo) at the given ratios (mean ± SEM). The percent suppression of PB Teffs from a common third-party control by Tregs (CD4+CD25+CD127lo) from the SF of a chronic sJIA patient at the given ratios is also depicted. **(D)** Heatmap depicting methylation rates of CpG sites in CNS2 of *FOXP3* in sorted Tregs (CD4+CD25+CD127lo) and Teffs (CD4+CD25−) from acute sJIA PB, chronic sJIA PB, chronic sJIA SF, and healthy control PB. Acute sJIA9, chronic sJIA 5, and HC Adult 4 are all males. **(E)** Mean percentage of methylation rates (mean ± SD) of all evaluated 9 CpG sites in CNS2 of *FOXP3* in sorted Tregs (CD4+CD25+CD127lo) and Teffs (CD4+CD25−) from acute sJIA PB (*n* = 5), chronic sJIA PB (*n* = 4), and healthy control PB (*n* = 5) (*t* tests, ***$P \leq 0.001$; ****$P \leq 0.0001$). Teff, T effector cell; D0, % nondividing cells; sJIA, systemic juvenile idiopathic arthritis; SF, synovial fluid; CNS2, conserved noncoding sequences 2.

and showed enhanced IL-17A expression in circulating γδ T cells (mean fluorescence intensity) without an overall expansion of the IL-17+ γδ T cell population (66). Patients with active sJIA exhibited an increase in serum IL-17A, and IL-1 blockade was associated with lower IL-17A expression in γδ T cells (66). Here, we provide the first comparison of T cells across acute and chronic sJIA, including close examination of Tregs, together with detailed transcriptomic profiling. We find that the Th17 response in sJIA evolves over time. Tregs are the first to exhibit a Th17 skew, remaining aberrant even in chronic sJIA, where an expanded population of activated Tregs appears in both blood and joints. However, in chronic arthritic disease, the Th17 signature is most evident in the Teff population — although, like Omoyinmi and Kessel (61, 66), we find that circulating Teffs expressing the cytokine IL-17A with conventional in vitro stimulation remain uncommon. Importantly, these Teffs do not demonstrate features of exhaustion, expressing IFN-γ at levels comparable with controls and increased transcription of genes related to proinflammatory cytokines, including TNF-α, IL-6, IFN-α, and IL-2 (Figure 3C and Figure 5C).

The findings presented here do not establish that the cell populations we observe are pathogenic. It remains possible that the sJIA cytokine milieu skews the distribution and phenotype of T cells but that these cells remain incidental to the development of chronic arthritis. However, evidence for their relevance comes from several sources. T cells polarized by IL-1 and IL-6 mediate murine inflammatory arthritis (37–39, 41, 67). In humans, the association between sJIA and HLA-DRB1*11 suggests a pathogenic role for CD4+ T cells, especially since the haplotype containing this allele is also associated with forms of arthritis beyond sJIA (27, 68, 69). The few examples of SF examined here place the activated, proliferative Treg population within the affected tissue, although unfortunately, these samples were too limited in quantity to evaluate
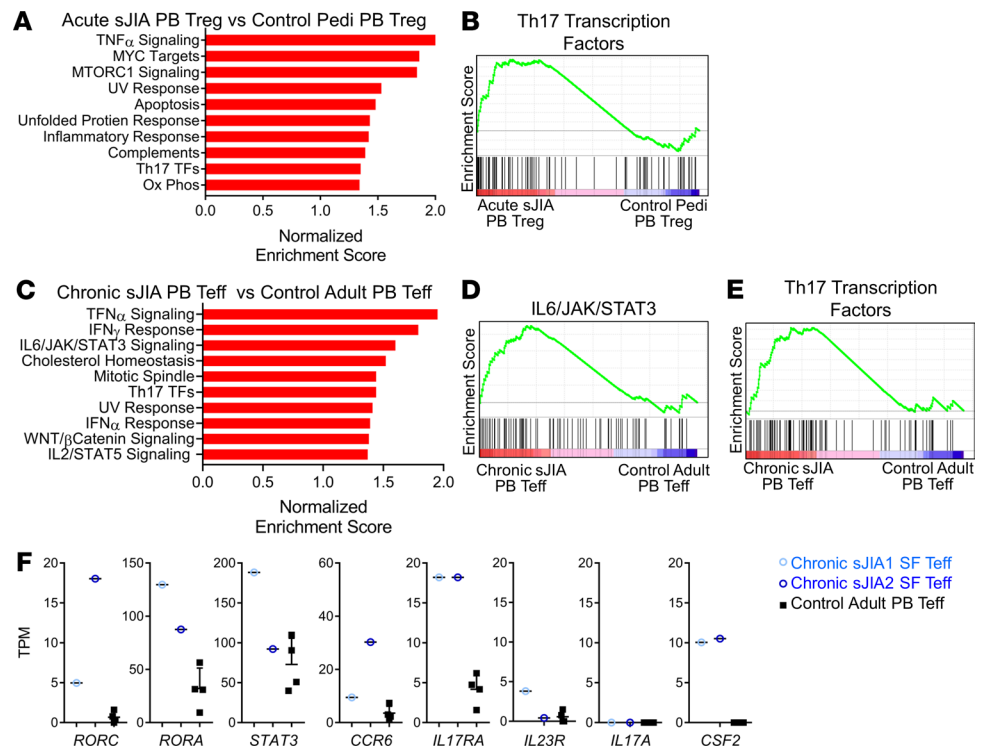
**Figure 5. Tregs in acute sJIA and Teffs in chronic sJIA demonstrate a Th17 gene expression signature.** (**A**) Top enriched gene sets in peripheral blood (PB) Tregs (CD4+CD25+CD127lo) from patients with acute sJIA (*n* = 8) compared with pediatric healthy controls (*n* = 3) based on the normalized enrichment score (NES) from Gene Set Enrichment Analysis (GSEA). (**B**) The enrichment plots of the Th17 transcription factor gene set from the GSEA in **A**. (**C**) Top enriched gene sets in PB Teffs (CD4+CD25−) from patients with chronic sJIA (*n* = 7) compared with adult healthy controls (*n* = 4) based on the NES from GSEA. (**D** and **E**) The enrichment plots of the IL-6/JAK/STAT3 and Th17 transcription factor gene sets from the GSEA in **C**. (**F**) RNA sequencing expression data for the given genes in PB Teffs from healthy adult controls (*n* = 4) (mean ± SD) and SF Teffs from 2 patients with chronic sJIA. All displayed gene sets have an FDR < 0.1. sJIA, systemic juvenile idiopathic arthritis; Pedi, pediatric; TF, transcription factor; Ox Phos, oxidative phosphorylation; Teff, effector T cell; TPM, transcripts per million; SF, synovial fluid

IL-17A production directly. Finally, clinical reports confirm that therapy directed against T cells can sometimes be effective in sJIA. In particular, chronic sJIA arthritis can respond to the T cell costimulation blocker abatacept, although IL-1β and IL-6 blockade also remain effective in established disease (70, 71).

The population of Tregs we observe here in sJIA, both acute and chronic, is particularly interesting. It expresses markers of memory (CD45RO), activation (HLADR, PD1, ICOS), and proliferation (Ki67), as well as Treg TFs (HELIOS) and Treg effector molecules (CTLA4, GITR, CD39). In new-onset sJIA patients, Tregs can express IL-17A, though Teffs, CD4+ memory cells, and γδ T cells do not (Figure 3). This phenomenon is specific for sJIA, as we do not identify similar circulating cytokine-expressing Tregs in children with other types of JIA.

In addition to Treg dysregulation, we highlight Th17 polarization in sJIA. IL-1β and IL-6 have profound effects on lymphocytes, promoting Th17 differentiation and impairing Treg fitness (29–36). While Th17-polarized T cells were most easily demonstrated in blood, Teffs from the available SF samples exhibited a similar signature, further supporting the possibility that they contribute pathogenically. Unlike mice with arthritis through absence of IL-1RA, we observe no enrichment for IL-17+ γδ T cells in either blood or joint (39). This finding echoes that of Kessel et al., though our data do not allow us to test their observation that per-cell IL-17A expression is enhanced in γδ T cells (66). The relative rarity of γδ17 T cells in sJIA could suggest that their role is less important than in the murine model. However, no data are yet available regarding γδ17 T cells within sJIA synovial tissues (rather than fluid), and we cannot exclude the possibility that even a small number of such cells could be pathophysiologically important. While our results showed increased Th17 polarization in CD4+ T cells, Th1 skewing was not observed. Interestingly, there is increasing evidence that IFN-γ and IFN-γ–inducible mediators (CXCL9, CXCL10, adenosine deaminase 2) are biomarkers that
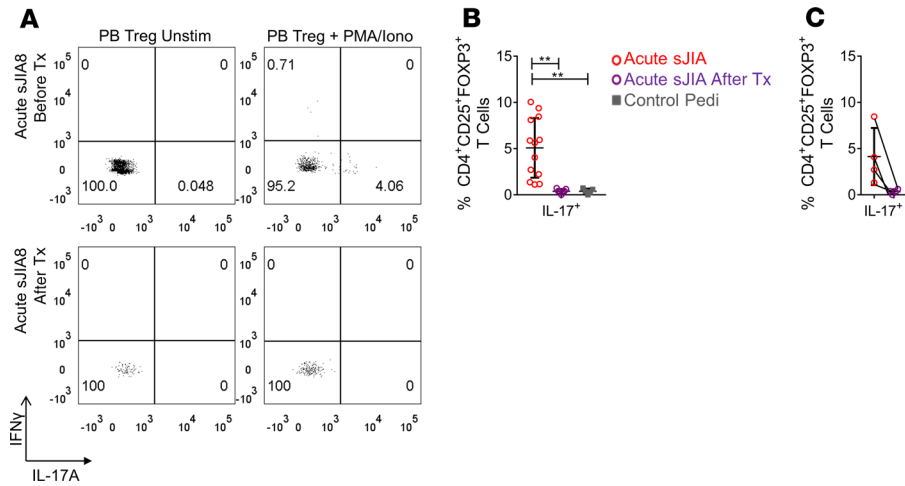
**Figure 6. The Th17 reprogramming of Tregs in sJIA is reversed in patients treated with first-line rIL-1RA.** (**A**) Representative flow cytometry dot plots gated on peripheral blood (PB) Tregs (CD4$^+$CD25$^+$FOXP3$^+$). (**B**) The mean percentage ± SD of IL-17$^+$ Tregs (CD4$^+$CD25$^+$FOXP3$^+$) in acute sJIA patients (*n* = 15) compared with patients treated with first-line rIL-1RA (within 4 weeks of diagnosis) who entered remission (*n* = 7). Pediatric controls are also depicted (*n* = 5). (**C**) The mean percentage ± SD of IL-17$^+$ Tregs (CD4$^+$CD25$^+$FOXP3$^+$) in 4 sJIA patients at disease onset and after remission was induced by first-line treatment with rIL-1RA (1-way ANOVA corrected for multiple comparisons, **$P \leq 0.01$). sJIA, systemic juvenile idiopathic arthritis; Tx, treatment; Unstim, unstimulated; PB, peripheral blood; Pedi, pediatric

differentiate between active sJIA and active sJIA with MAS (72–74). In our study, a majority of patients had active sJIA without MAS, and this may explain the lack of Th1/IFN-γ signal in this cohort (Table 1).

The shift in Th17 response from Tregs in acute disease to Teffs in chronic disease is reminiscent of other examples of cytokine-mediated Treg conversion. In collagen-induced arthritis, Komatsu and collaborators showed that IL-6 generated by synovial fibroblasts drives Tregs to express IL-17 and CCR6 and thereby become bona fide Th17 cells (i.e., ex-Tregs) (41). Komatsu et al. postulated that these exFOXP3 Th17 cells may be especially pathogenic because the T cell receptor repertoire of Tregs is more likely to recognize self-antigens. A similar phenomenon occurs in patients with asthma who carry the Q576R polymorphism in the IL-4Rα chain. This mutant IL-4 receptor activates IL-6 and STAT3 signaling, mediating Treg conversion into Th17 cells and thereby contributing to severe refractory asthma (75). Studies in murine and human cells demonstrate that IL-1β induces IL-17 expression in Tregs (33, 36). We speculate that the cytokine environment in acute sJIA distorts the Treg population, including induction of IL-17 expression. These Tregs may contribute to arthritis. Whether they also convert into FOXP3$^−$ Th17 effector cells remains to be determined. Lineage tracing of Tregs in sJIA patients to document this conversion is likely infeasible, so further studies in animal models will be required to test this possibility.

Our data are consistent with the biphasic hypothesis of sJIA, whereby cytokines in the acute phase of sJIA help to unleash a chronic autoimmune arthritis driven by adaptive immunity (21, 28). We show here that adaptive immune dysfunction in sJIA is evident first in Tregs, suggesting that they may be particularly vulnerable to the IL-1β– and IL-6–rich environment of acute sJIA. If this hypothesis is correct, treatment aimed at restoring immune tolerance in Tregs with medications such as abatacept (CTLA4-Ig), low dose IL-2, or rapamycin could have a clinical role, especially near disease onset. Blockade of IL-1 or IL-6 could also exert such a function. Patients with sJIA and chronic arthritis may respond to medications that target Th17 cells, an approach yet to be attempted in this disease. Further studies are required to evaluate the therapeutic efficacy of targeting T cells in sJIA.

Taken a step further, the biphasic hypothesis suggests that there may be a "window of opportunity" to treat sJIA patients early in the disease course (21). By forestalling Th17 polarization, cytokine blockade at disease onset might abrogate progression to chronic arthritis. Indeed, we show that IL-1 blockade within the first month of disease onset abolished IL-17A expression in Tregs, in keeping with findings that such treatment correlates with lower rates of chronic arthritis in sJIA (22, 23, 26). Historical reports found that 50%–60% of patients with sJIA develop uncontrolled chronic arthritis (4, 5). By contrast, over 90% of sJIA patients receiving first-line IL-1 blockade achieve inactive disease (26). Further work is needed to clarify the role of up-front

cytokine blockade in preventing Treg dysfunction, Th17 polarization, and chronic arthritis in sJIA, as well as to establish the safety of this approach — in particular, with respect to sJIA-associated lung disease (76–78).

The results of this study must be interpreted within the context of the complexities of human research in a rare pediatric disease. Patients exhibit considerable heterogeneity, especially in chronic long-standing disease with years of immunomodulatory treatment. Ideally, patients should be studied off medications, but this was often not possible, given the acuity and severity of sJIA. By analyzing patients with acute and chronic sJIA and comparing them with pediatric and adult controls, we sought to account for some of this variability. While the capacity of IL-1β and IL-6 to skew T cells toward a Th17 phenotype is well documented, our studies do not demonstrate that these cytokines directly drive Treg dysfunction and Th17 polarization in sJIA. It is possible that sJIA patients have an intrinsic Treg, T cell, or other defect that enables the autoinflammatory phase of sJIA to occur in the first place, and then for these cells to become pathogenic. Indeed, heterogeneity within sJIA suggests that underlying mechanisms likely vary between patients (79).

The function of IL-17+ Tregs remains to be clarified. We show that bulk Tregs maintain suppressive function in vitro, but these studies do not necessarily reflect in vivo suppressive capacity because they do not capture the effect of Tregs on target populations other than proliferating T cells, such as antigen-presenting cells and monocytes, which may be of particular importance in sJIA (80). Furthermore, in vitro assays evaluate the activity of the Treg population as a whole, rather than of subpopulations such as IL-17+ Tregs. Whether the sJIA Tregs observed here are in fact pathogenic, thus, requires further investigation.

Innate and adaptive immunity exhibit close interconnection at many levels, and it is therefore highly plausible that disease originating within one "arm" of immunity could trigger pathogenic changes in the other. By studying sJIA stratified by disease duration, we show polarization of T cells toward a Th17 phenotype in sJIA. This process is first observed in Tregs, progressing to Teffs in both blood and SF in patients who go on to develop chronic arthritis. These results suggest potentially novel treatment strategies for patients with sJIA, including early initiation of cytokine blockade to prevent T cell reprograming, interventions to augment Treg fitness, and — potentially — therapies directed against the Th17 pathway.

## Methods

*Patients*. Patients with sJIA and nonsystemic forms of JIA, as defined by International League of Associations for Rheumatology (ILAR) criteria, were recruited from the Rheumatology Clinics at Boston Children's Hospital (BCH), Brigham and Women's Hospital (BWH), and Children's of Alabama Hospital (University of Alabama at Birmingham, UAB) (2). All sJIA patients had arthritis. Children with sJIA for less than 4 months with ongoing fevers, arthritis, and elevated ESR and/or CRP were classified as acute-onset sJIA patients. Chronic sJIA was defined by disease duration longer than 6 months and persistent arthritis. Healthy controls with noninflammatory causes of joint pain were recruited from the BCH Rheumatology Clinic. Peripheral blood samples and, when possible, discard SF samples from a diagnostic or therapeutic joint aspiration were obtained from the enrolled participants. Medical records were reviewed by a board-certified pediatric rheumatologist to confirm the arthritis diagnosis and to obtain the relevant clinical data.

*Cell isolation*. Mononuclear cells from blood and SF were isolated by Ficoll density gradient centrifugation (GE Healthcare). For flow cytometry, fluorescence-activated cell sorting, and functional assays, all samples were frozen and thawed in the same manner. The isolated PBMCs and SFMCs were cryopreserved in liquid nitrogen and then thawed into RMPI (HyClone) with 10% FBS (MilliporeSigma), penicillin 100 IU/mL (Corning Cellgro), streptomycin 100 μg/mL (Corning Cellgro), nonessential amino acids (Corning Cellgro), sodium pyruvate 1 mM (Corning Cellgro), and HEPES 10 mM (Thermo Fisher Scientific) and rested overnight for subsequent downstream analyses.

*Mass cytometry*. All samples used for mass cytometry were thawed in a 37°C water bath for 3 minutes and then mixed with 37°C thawing media containing RPMI Medium 1640 (Invitrogen) supplemented with 5% heat-inactivated FBS (Invitrogen), 1 mM GlutaMAX Supplement (Invitrogen), antibiotic-antimycotic (Invitrogen), 2 mM MEM nonessential amino acids (Invitrogen ), 10 mM HEPES (Invitrogen), $2.5 \times 10^{-5}$ M 2-mercaptoethanol (Sigma-Aldrich), 20 units/mL sodium heparin (Sigma-Aldrich), and 25 units/mL benzonase nuclease (Sigma-Aldrich). Approximately $1.5 \times 10^6$ cells were used form each sample and transferred to a tissue culture plate and rested in culture media (thawing media excluding sodium heparin and benzonase nuclease) for 30 minutes at 37°C. Samples were spun down and aspirated, before 5 μM of cisplatin viability staining reagent (Fluidigm) was added for 2 minutes and then diluted with culture media.

After centrifugation, Human TruStain FcX Fc receptor blocking reagent (BioLegend) was used at a 1:100 dilution in CSB (PBS with 2.5 g BSA [Sigma Aldrich] and 100 mg of sodium azide [Sigma Aldrich]) for 10 minutes, followed by incubation with conjugated surface antibodies (each marker was used at a 1:100 dilution in CSB) for 30 minutes. Antibodies conjugated to heavy metals were obtained from Fluidigm and the Longwood Medical Area CyTOF Antibody Resource Core, an affiliate of the Joint Biology Consortium (www.jbcwebportal.org). The Longwood Medical Area CyTOF Antibody Resource Core conjugated antibodies to metal-chelated polymers, per the protocol detailed in the MaxPar Antibody Labeling Kit provided by Fluidigm. A 16% stock paraformaldehyde (Thermo Fisher Scientific) dissolved in PBS was used at a final concentration of 4% for 10 minutes to fix the samples before permeabilization with the FOXP3/Transcription Factor Staining Buffer Set (Thermo Fisher Scientific). The samples were incubated with palladium barcoding reagents (Fluidigm) for 15 minutes and then combined into 2 final samples. Conjugated intracellular antibodies (each marker was used at a 1:100 dilution, except for FOXP3, which was used at 1:50) was added into each tube and incubated for 30 minutes. A final light fixation with 16% stock paraformaldehyde used at 1.6% was added to the samples for 10 minutes. To stain for DNA, 18.75 µM iridium intercalator solution (Fluidigm) was added to the samples for 20 minutes. Samples were subsequently washed and reconstituted in Milli-Q filtered distilled water with EQ Four Element Calibration beads (Fluidigm) and then run on a Helios CyTOF Mass Cytometer (Fluidigm). In total, 2 mass cytometry runs were performed, and samples from acute and chronic sJIA, as well as pediatric and adult controls, were included in each run. The raw FCS files were first normalized to reduce deviation between signals over the course of multiday batch acquisitions utilizing the bead standard normalization method established by Finck et al. (81). The normalized files were then debarcoded into individual sample files using a single-cell based debarcoding algorithm established by Zunder et al. (82).

Cytobank (https://www.cytobank.org) was used to perform viSNE and SPADE analyses. viSNE analysis of live ($^{195}Pt^-$), single ($^{191}Ir^+$, $^{193}Ir^+$) cells from paired samples PB and SF samples ($n = 2$) was done with proportional sampling and based on all measured protein markers (Supplemental Table 1). CD4 and CD8 naive and memory T cells, Tregs, and γδ T cells were manually gated onto the viSNE plots in Cytobank. Gated live single Tregs ($CD4^+CD25^+CD127^{lo}$) from these paired samples were also evaluated with viSNE (PB and SF from the same patient were evaluated in a single viSNE run) with all parameters in Supplemental Table 1 used for the analysis, except those required for gating the Treg population ($CD3^+$, $CD4^+$, $CD8^+$, T cell receptor γδ$^+$, $CD25^+$, $CD127^{lo}$).

For concatenated analysis, all samples, were gated on live single Tregs ($CD4^+CD25^+CD127^{lo}$) or memory $CD4^+$ T cells ($CD4^+CD45RO^+$ after Tregs were gated out of the analysis) (acute sJIA PB, $n = 6$; chronic sJIA PB, $n = 4$; chronic sJIA SF, $n = 2$; and healthy controls, $n = 6$) and evaluated in a single viSNE analysis using equal sampling and all cytometric parameters except those required for gating Tregs or $CD4^+$ memory T cells. The resulting output files were concatenated by study subject group with Cytobank tools and then exported as FCS files into FlowJo to evaluate expression of cell markers. For SPADE analysis, the concatenated files were used with the following settings: target of 50 nodes (informed by VorteX, https://github.com/nolanlab/vortex/releases; https://github.com/nolanlab/vortex/releases/tag/26-Apr-2018) and downsampling of 10%. All cytometric parameters were used for the analysis, except those required for gating Tregs. The SPADE trees were visually inspected, and the bubble tool was used to identify the largest cluster of SF Tregs. Statistical data from each SPADE tree were downloaded from Cytobank to determine the frequency of events. Cytobank-generated FCS files from the created SPADE bubbles were exported into FlowJo to evaluate the expression of cell markers in this population.

*Flow cytometry.* PBMCs and SFMCs were left unstimulated or simulated with a cocktail of PMA, ionomycin, and Brefeldin (BD Biosciences) and stained with the following antibodies: anti–CD4-FITC (RPA-T4, BD Biosciences, catalog 555346), anti–CD25-PE (BC96, eBioscience, catalog 12-0259-42), anti–CD127-PECy7 (A019D5, BioLegend, catalog 351320), anti–CD45RO-FITC (UCHL1, BioLegend, catalog 304204), anti–CD4-PE (OKT4, BioLegend, catalog 317410), anti–CD3-PECy7 (OKT3, BioLegend, catalog 317334), and anti–Tgd-FITC (B1.1, eBioscience, catalog 11-9959-42). After cell surface staining, cells were fixed, permeabilized (eBiosciences), and stained with anti–CTLA4-APC (L3D10, BioLegend, catalog 349908), anti–HELIOS–PerCp-Cy5.5 (22F6, BioLegend, catalog 137230), anti–FOXP3–pacific blue (PCH101, Invitrogen, catalog 48-4776-42), anti–IFN-γ–APC (4S.B3, BioLegend, catalog 502512), and anti–IL-17A–PerCp-Cy5.5 (BL168, BioLegend, catalog 512314). Data was acquired on a LSRFortessa (BD Biosciences) and analyzed by FlowJo.

*Treg suppression assays.* FACS was used to isolate Tregs (CD4$^+$CD25$^+$CD127$^{lo}$) and Teffs (CD4$^+$CD25$^-$). The suppressive capacity of Tregs was tested against Teffs from a common third-party control. Teffs were labeled with CellTrace Violet (Invitrogen) and stimulated with anti-CD2/CD3/CD28 beads (Miltenyi Biotec). The labeled Teffs were cocultured with Tregs in U-bottom plates at 1:1, 2:1, 4:1, and 8:1 ratios. After 4 days, cell division of Teffs was measured by dye dilution through flow cytometry (LSRFortessa, BD Biosciences).

*CpG methylation analysis.* Tregs (CD4$^+$CD25$^+$CD127$^{lo}$) and Teffs (CD4$^+$CD25$^-$) were isolated by FACS. Sorted cells were pelleted, snap frozen in liquid nitrogen, and stored at –80°C. DNA extraction, bisulfite conversion, pyrosequencing, and data analysis were done by EpigenDx, as published previously (83, 84). Nine cytosine guanine dinucleotides (CpGs) of the human Treg–specific demethylation region (CNS2 of *FOXP3*) were analyzed (–2330 to –2263 from ATG translational start codon).

*RNA-seq.* RNA was extract from sorted Tregs (CD4$^+$CD25$^+$CD127$^{lo}$) and Teffs (CD4$^+$CD25$^-$) (10,000 cells) from the PB of acute sJIA (*n* = 8), chronic sJIA (*n* = 7), pediatric control (*n* = 5), and adult control (*n* = 4) study subjects, as well as the SF of 2 patients with chronic sJIA (Qiagen). RNA-seq was performed using the Smart-seq2 platform at the Broad Technology Labs, which supports full-length transcript sequencing from low cell inputs (85–87). Smart-seq2 libraries were prepared and sequenced using an Illumina NextSeq500. Sequencing was done in 2 technical batches, with identical pipelines run on each. To assess whether there was any resultant confounding batch effect, principal component analysis (PCA) was performed on full gene expression profiles, overlayed with batch annotations, to enable determination if batches were driving clusters over and above any biological factors. There appeared to be even, overlapping spread of both run1 and run2 samples in the PCA and, therefore, batch effects were not significant.

All samples were analyzed using the bcbio-nextgen RNA-seq analysis pipeline (https://bcbio-nextgen.readthedocs.org/en/latest/). BAM files were converted back to fastq read files and were examined for quality issues using FastQC (http://www.bioinformatics.babraham.ac.uk/projects/fastqc/) to ensure library generation and sequencing were suitable for further analysis. Adapter sequences and other contaminant sequences such as polyA tails and low-quality sequences with PHRED quality scores less than 5 were trimmed from reads using atropos (https://github.com/jdidion/atropos) where necessary. Trimmed reads were aligned to UCSC build GRCh37 of the human genome (homo sapiens), augmented with transcript information from Ensembl release 90, using STAR (88). Alignments were checked for evenness of coverage, rRNA content, genomic context of alignments, complexity, and other quality checks using a combination of FastQC, Qualimap (89), MultiQC (https://github.com/ewels/MultiQC), and custom tools. Counts of reads aligning to known genes were generated by featureCounts (90). In parallel, transcripts per million (TPM) measurements per isoform were generated by quasialignment using Salmon (91). Differential expression at the gene level was determined with DESeq2 (92) preferring to use counts per gene estimated from the Salmon quasialignments by tximport (93). A cut-off–free GSEA was performed using software from the Broad Institute with the hallmark gene sets of the Molecular Signatures Database (MsigDB) (94–96), the human Treg gene set sourced from Ferraro et al. (60), and the Th17 TF gene set obtained from Ciofani et al. (57). The RNA-seq data supporting this publication are available at ImmPort (https://www.immport.org) under study accession SDY1591.

*Statistics.* Differences in frequency of T cells expressing a given cell surface marker, TF, or intracellular cytokine as measured by flow cytometry were evaluated across > 2 study subject groups with 1-way ANOVA and the Sidak's correction for multiple comparisons. The Mann Whitney *U* test was used to compare CCR6 expression in acute sJIA vs. pediatric control PB Tregs. The relationship between CCR6 and IL-17 expression in Tregs was evaluated with the Spearman's correlation coefficient. Global CpG methylation was compared in Treg and Teffs with 2-tailed Student's *t* test. For these statistical studies, a *P* value less than 0.05 was considered significant. GraphPad Prism version 7.0 was used for the statistical analysis. For GSEA analysis, significance was defined at an FDR < 10%.

*Study approval.* This study was performed in accordance with the IRBs at BCH, BWH, and UAB. Written informed consent (and assent when appropriate) from the participants was obtained.

## Author contributions

LAH conceptualized and performed research, recruited patients, analyzed data, and wrote the manuscript. KJH recruited patients, performed flow cytometry and methylation experiments, and analyzed the resulting data. PYL, KR, and CN assisted in RNA-seq experiments and analysis. DAR designed the mass cytometry panel. AHJ assisted in mass cytometry data analysis. AMJ and LMC assisted with in vitro experiments. JPN and JAL provided reagents and performed mass cytometry experiments. SC, MHC, EMC, FD,

Address correspondence to: Peter A. Nigrovic, 60 Fenwood Road, Hale Building for Transformative Medicine, Room 6002L, Boston, Massachusetts 02115, USA. Phone: 617.525.1031; Email: pnigrovic@bwh.harvard.edu.

KR's present address is: Center for Hematologic Malignancies, Memorial Sloan Kettering Cancer Center, New York, USA.

EMC's present address is: Department of Pediatrics, Boston Medical Center, Boston, Massachusetts, USA.

RCF's present address is: Pediatric Rheumatology, Children's Hospital of Colorado, Aurora, Colorado, USA.

SK's present address is: Pediatric Rheumatology, Benioff Children's Hospital, San Francisco, California, USA.

CN's present address is: Cellarity Inc., Cambridge, Massachusetts, USA.

1. Still GF. On a Form of Chronic Joint Disease in Children. *Med Chir Trans*. 1897;80:47–60.9.
2. Petty RE, et al. International League of Associations for Rheumatology classification of juvenile idiopathic arthritis: second revision, Edmonton, 2001. *J Rheumatol*. 2004;31(2):390–392.
3. Behrens EM, et al. Evaluation of the presentation of systemic onset juvenile rheumatoid arthritis: data from the Pennsylvania Systemic Onset Juvenile Arthritis Registry (PASOJAR). *J Rheumatol*. 2008;35(2):343–348.
4. Singh-Grewal D, Schneider R, Bayer N, Feldman BM. Predictors of disease course and remission in systemic juvenile idiopathic arthritis: significance of early clinical and laboratory features. *Arthritis Rheum*. 2006;54(5):1595–1601.
5. Lomater C, Gerloni V, Gattinara M, Mazzotti J, Cimaz R, Fantini F. Systemic onset juvenile idiopathic arthritis: a retrospective study of 80 consecutive patients followed for 10 years. *J Rheumatol*. 2000;27(2):491–496.
6. Janow G, et al. The Systemic Juvenile Idiopathic Arthritis Cohort of the Childhood Arthritis and Rheumatology Research Alliance Registry: 2010-2013. *J Rheumatol*. 2016;43(9):1755–1762.
7. Packham JC, Hall MA. Long-term follow-up of 246 adults with juvenile idiopathic arthritis: functional outcome. *Rheumatology (Oxford)*. 2002;41(12):1428–1435.
8. Mellins ED, Macaubas C, Grom AA. Pathogenesis of systemic juvenile idiopathic arthritis: some answers, more questions. *Nat Rev Rheumatol*. 2011;7(7):416–426.
9. Martini A, et al. Toward New Classification Criteria for Juvenile Idiopathic Arthritis: First Steps, Pediatric Rheumatology International Trials Organization International Consensus. *J Rheumatol*. 2019;46(2):190–197.
10. Macaubas C, et al. Alternative activation in systemic juvenile idiopathic arthritis monocytes. *Clin Immunol*. 2012;142(3):362–372.
11. Macaubas C, et al. Altered signaling in systemic juvenile idiopathic arthritis monocytes. *Clin Immunol*. 2016;163:66–74.
12. Cepika AM, et al. A multidimensional blood stimulation assay reveals immune alterations underlying systemic juvenile idiopathic arthritis. *J Exp Med*. 2017;214(11):3449–3466.
13. Ter Haar NM, et al. Reversal of Sepsis-Like Features of Neutrophils by Interleukin-1 Blockade in Patients With Systemic-Onset Juvenile Idiopathic Arthritis. Arthritis Rheumatol. 2018;70(6):943–956.
14. Villanueva J, et al. Natural killer cell dysfunction is a distinguishing feature of systemic onset juvenile rheumatoid arthritis and macrophage activation syndrome. *Arthritis Res Ther*. 2005;7(1):R30–R37.

15. Frosch M, et al. The myeloid-related proteins 8 and 14 complex, a novel ligand of toll-like receptor 4, and interleukin-1beta form a positive feedback mechanism in systemic-onset juvenile idiopathic arthritis. *Arthritis Rheum*. 2009;60(3):883–891.

16. de Jager W, et al. Defective phosphorylation of interleukin-18 receptor beta causes impaired natural killer cell function in systemic-onset juvenile idiopathic arthritis. *Arthritis Rheum*. 2009;60(9):2782–2793.

17. Pascual V, Allantaz F, Arce E, Punaro M, Banchereau J. Role of interleukin-1 (IL-1) in the pathogenesis of systemic onset juvenile idiopathic arthritis and clinical response to IL-1 blockade. *J Exp Med*. 2005;201(9):1479–1486.

18. Ruperto N, et al. Two randomized trials of canakinumab in systemic juvenile idiopathic arthritis. *N Engl J Med*. 2012;367(25):2396–2406.

19. De Benedetti F, et al. Randomized trial of tocilizumab in systemic juvenile idiopathic arthritis. *N Engl J Med*. 2012;367(25):2385–2395.

20. Gabay C, et al. Open-label, multicentre, dose-escalating phase II clinical trial on the safety and efficacy of tadekinig alfa (IL-18BP) in adult-onset Still's disease. *Ann Rheum Dis*. 2018;77(6):840–847.

21. Nigrovic PA. Review: is there a window of opportunity for treatment of systemic juvenile idiopathic arthritis? *Arthritis Rheumatol*. 2014;66(6):1405–1413.

22. Nigrovic PA, et al. Anakinra as first-line disease-modifying therapy in systemic juvenile idiopathic arthritis: report of forty-six patients from an international multicenter series. *Arthritis Rheum*. 2011;63(2):545–555.

23. Vastert SJ, et al. Effectiveness of first-line treatment with recombinant interleukin-1 receptor antagonist in steroid-naive patients with new-onset systemic juvenile idiopathic arthritis: results of a prospective cohort study. *Arthritis Rheumatol*. 2014;66(4):1034–1043.

24. Quartier P, et al. A multicentre, randomised, double-blind, placebo-controlled trial with the interleukin-1 receptor antagonist anakinra in patients with systemic-onset juvenile idiopathic arthritis (ANAJIS trial). *Ann Rheum Dis*. 2011;70(5):747–754.

25. Pardeo M, et al. Anakinra in Systemic Juvenile Idiopathic Arthritis: A Single-center Experience. *J Rheumatol*. 2015;42(8):1523–1527.

26. Ter Haar NM, et al. Treatment to Target Using Recombinant Interleukin-1 Receptor Antagonist as First-Line Monotherapy in New-Onset Systemic Juvenile Idiopathic Arthritis: Results From a Five-Year Follow-Up Study. *Arthritis Rheumatol*. 2019;71(7):1163–1173.

27. Ombrello MJ, et al. HLA-DRB1*11 and variants of the MHC class II locus are strong risk factors for systemic juvenile idiopathic arthritis. *Proc Natl Acad Sci USA*. 2015;112(52):15970–15975.

28. Nigrovic PA. Autoinflammation and autoimmunity in systemic juvenile idiopathic arthritis. *Proc Natl Acad Sci USA*. 2015;112(52):15785–15786.

29. Zielinski CE, et al. Pathogen-induced human TH17 cells produce IFN-γ or IL-10 and are regulated by IL-1β. *Nature*. 2012;484(7395):514–518.

30. Yang L, et al. IL-21 and TGF-beta are required for differentiation of human T(H)17 cells. *Nature*. 2008;454(7202):350–352.

31. Li MO, Sanjabi S, Flavell RA. Transforming growth factor-beta controls development, homeostasis, and tolerance of T cells by regulatory T cell-dependent and -independent mechanisms. *Immunity*. 2006;25(3):455–471.

32. Zhou L, et al. IL-6 programs T(H)-17 cell differentiation by promoting sequential engagement of the IL-21 and IL-23 pathways. *Nat Immunol*. 2007;8(9):967–974.

33. Koenen HJ, Smeets RL, Vink PM, van Rijssen E, Boots AM, Joosten I. Human CD25highFoxp3pos regulatory T cells differentiate into IL-17-producing cells. *Blood*. 2008;112(6):2340–2352.

34. Deknuydt F, Bioley G, Valmori D, Ayyoub M. IL-1beta and IL-2 convert human Treg into T(H)17 cells. *Clin Immunol*. 2009;131(2):298–307.

35. Gagliani N, et al. Th17 cells transdifferentiate into regulatory T cells during resolution of inflammation. *Nature*. 2015;523(7559):221–225.

36. Li L, Kim J, Boussiotis VA. IL-1β-mediated signals preferentially drive conversion of regulatory T cells but not conventional T cells into IL-17-producing cells. *J Immunol*. 2010;185(7):4148–4153.

37. Horai R, et al. Development of chronic inflammatory arthropathy resembling rheumatoid arthritis in interleukin 1 receptor antagonist-deficient mice. *J Exp Med*. 2000;191(2):313–320.

38. Koenders MI, et al. Interleukin-1 drives pathogenic Th17 cells during spontaneous arthritis in interleukin-1 receptor antagonist-deficient mice. *Arthritis Rheum*. 2008;58(11):3461–3470.

39. Akitsu A, et al. IL-1 receptor antagonist-deficient mice develop autoimmune arthritis due to intrinsic activation of IL-17-producing CCR2(+)Vγ6(+)γδ T cells. *Nat Commun*. 2015;6:7464.

40. Morgan ME, et al. Effective treatment of collagen-induced arthritis by adoptive transfer of CD25+ regulatory T cells. *Arthritis Rheum*. 2005;52(7):2212–2221.

41. Komatsu N, et al. Pathogenic conversion of Foxp3+ T cells into TH17 cells in autoimmune arthritis. *Nat Med*. 2014;20(1):62–68.

42. van Hamburg JP, Tas SW. Molecular mechanisms underpinning T helper 17 cell heterogeneity and functions in rheumatoid arthritis. *J Autoimmun*. 2018;87:69–81.

43. Taams LS, Steel KJA, Srenathan U, Burns LA, Kirkham BW. IL-17 in the immunopathogenesis of spondyloarthritis. *Nat Rev Rheumatol*. 2018;14(8):453–466.

44. de Kleer IM, et al. CD4+CD25bright regulatory T cells actively regulate inflammation in the joints of patients with the remitting form of juvenile idiopathic arthritis. *J Immunol*. 2004;172(10):6435–6443.

45. Haufe S, et al. Impaired suppression of synovial fluid CD4+CD25- T cells from patients with juvenile idiopathic arthritis by CD4+CD25+ Treg cells. *Arthritis Rheum*. 2011;63(10):3153–3162.

46. Wehrens EJ, et al. Functional human regulatory T cells fail to control autoimmune inflammation due to PKB/c-akt hyperactivation in effector cells. *Blood*. 2011;118(13):3538–3548.

47. Henderson LA, et al. Next-Generation Sequencing Reveals Restriction and Clonotypic Expansion of Treg Cells in Juvenile Idiopathic Arthritis. *Arthritis Rheumatol*. 2016;68(7):1758–1768.

48. Nistala K, Moncrieffe H, Newton KR, Varsani H, Hunter P, Wedderburn LR. Interleukin-17-producing T cells are enriched in the joints of children with arthritis, but have a reciprocal relationship to regulatory T cell numbers. *Arthritis Rheum*. 2008;58(3):875–887.

49. Amir el-AD, et al. viSNE enables visualization of high dimensional single-cell data and reveals phenotypic heterogeneity of

leukemia. *Nat Biotechnol*. 2013;31(6):545–552.

50. Thornton AM, et al. Expression of Helios, an Ikaros transcription factor family member, differentiates thymic-derived from peripherally induced Foxp3+ T regulatory cells. *J Immunol*. 2010;184(7):3433–3441.

51. Himmel ME, MacDonald KG, Garcia RV, Steiner TS, Levings MK. Helios+ and Helios- cells coexist within the natural FOXP3+ T regulatory cell subset in humans. *J Immunol*. 2013;190(5):2001–2008.

52. Sebastian M, Lopez-Ocasio M, Metidji A, Rieder SA, Shevach EM, Thornton AM. Helios Controls a Limited Subset of Regulatory T Cell Functions. *J Immunol*. 2016;196(1):144–155.

53. Baine I, Basu S, Ames R, Sellers RS, Macian F. Helios induces epigenetic silencing of IL2 gene expression in regulatory T cells. *J Immunol*. 2013;190(3):1008–1016.

54. Kim HJ, et al. Stable inhibitory activity of regulatory T cells requires the transcription factor Helios. *Science*. 2015;350(6258):334–339.

55. Ravelli A, et al. 2016 Classification Criteria for Macrophage Activation Syndrome Complicating Systemic Juvenile Idiopathic Arthritis: A European League Against Rheumatism/American College of Rheumatology/Paediatric Rheumatology International Trials Organisation Collaborative Initiative. *Arthritis Rheumatol*. 2016;68(3): 566–576.

56. Duhen T, Duhen R, Lanzavecchia A, Sallusto F, Campbell DJ. Functionally distinct subsets of human FOXP3+ Treg cells that phenotypically mirror effector Th cells. *Blood*. 2012;119(19):4430–4440.

57. Ciofani M, et al. A validated regulatory network for Th17 cell specification. *Cell*. 2012;151(2):289–303.

58. Yang XO, et al. T helper 17 lineage differentiation is programmed by orphan nuclear receptors ROR alpha and ROR gamma. *Immunity*. 2008;28(1):29–39.

59. Lazarevic V, et al. T-bet represses T(H)17 differentiation by preventing Runx1-mediated activation of the gene encoding RORγt. *Nat Immunol*. 2011;12(1):96–104.

60. Ferraro A, et al. Interindividual variation in human T regulatory cells. *Proc Natl Acad Sci USA*. 2014;111(12):E1111–E1120.

61. Omoyinmi E, et al. Th1 and Th17 cell subpopulations are enriched in the peripheral blood of patients with systemic juvenile idiopathic arthritis. *Rheumatology (Oxford)*. 2012;51(10):1881–1886.

62. Codarri L, et al. RORγt drives production of the cytokine GM-CSF in helper T cells, which is essential for the effector phase of autoimmune neuroinflammation. *Nat Immunol*. 2011;12(6):560–567.

63. El-Behi M, et al. The encephalitogenicity of T(H)17 cells is dependent on IL-1- and IL-23-induced production of the cytokine GM-CSF. *Nat Immunol*. 2011;12(6):568–575.

64. Raffin C, Raimbaud I, Valmori D, Ayyoub M. Ex vivo IL-1 receptor type I expression in human CD4+ T cells identifies an early intermediate in the differentiation of Th17 from FOXP3+ naive regulatory T cells. *J Immunol*. 2011;187(10):5196–5202.

65. Wallace CA, et al. American College of Rheumatology provisional criteria for defining clinical inactive disease in select categories of juvenile idiopathic arthritis. *Arthritis Care Res (Hoboken)*. 2011;63(7):929–936.

66. Kessel C, et al. Proinflammatory Cytokine Environments Can Drive Interleukin-17 Overexpression by gamma/delta T Cells in Systemic Juvenile Idiopathic Arthritis. *Arthritis Rheumatol*. 2017;69(7):1480–1494.

67. Nakae S, Saijo S, Horai R, Sudo K, Mori S, Iwakura Y. IL-17 production from activated T cells is required for the spontaneous development of destructive arthritis in mice deficient in IL-1 receptor antagonist. *Proc Natl Acad Sci USA*. 2003;100(10):5986–5990.

68. Thomson W, et al. Juvenile idiopathic arthritis classified by the ILAR criteria: HLA associations in UK patients. *Rheumatology (Oxford)*. 2002;41(10):1183–1189.

69. Hollenbach JA, et al. Juvenile idiopathic arthritis and HLA class I and class II interactions and age-at-onset effects. *Arthritis Rheum*. 2010;62(6):1781–1791.

70. Ruperto N, et al. Abatacept in children with juvenile idiopathic arthritis: a randomised, double-blind, placebo-controlled withdrawal trial. *Lancet*. 2008;372(9636):383–391.

71. Record JL, Beukelman T, Cron RQ. Combination therapy of abatacept and anakinra in children with refractory systemic juvenile idiopathic arthritis: a retrospective case series. *J Rheumatol*. 2011;38(1):180–181.

72. Bracaglia C, et al. Elevated circulating levels of interferon-γ and interferon-γ-induced chemokines characterise patients with macrophage activation syndrome complicating systemic juvenile idiopathic arthritis. *Ann Rheum Dis*. 2017;76(1):166–172.

73. Put K, et al. Cytokines in systemic juvenile idiopathic arthritis and haemophagocytic lymphohistiocytosis: tipping the balance between interleukin-18 and interferon-γ. *Rheumatology (Oxford)*. 2015;54(8):1507–1517.

74. Lee PY, et al. Adenosine deaminase 2 as a biomarker of macrophage activation syndrome in systemic juvenile idiopathic arthritis. *Ann Rheum Dis*. 2020;79(2):225–231.

75. Massoud AH, Charbonnier LM, Lopez D, Pellegrini M, Phipatanakul W, Chatila TA. An asthma-associated IL4R variant exacerbates airway inflammation by promoting conversion of regulatory T cells to TH17-like cells. *Nat Med*. 2016;22(9):1013–1022.

76. Kimura Y, et al. Pulmonary hypertension and other potentially fatal pulmonary complications in systemic juvenile idiopathic arthritis. *Arthritis Care Res (Hoboken)*. 2013;65(5):745–752.

77. Schulert GS, et al. Systemic Juvenile Idiopathic Arthritis-Associated Lung Disease: Characterization and Risk Factors. *Arthritis Rheumatol*. 2019;71(11):1943–1954.

78. Saper VE, et al. Emergent high fatality lung disease in systemic juvenile arthritis. *Ann Rheum Dis*. 2019;78(12):1722–1731.

79. Nigrovic PA, Raychaudhuri S, Thompson SD. Genetics and the classification of arthritis in adults and children. *Arthritis Rheumatol*. 2018;70(1):7–17.

80. Shevach EM. Foxp3+ T Regulatory Cells: Still Many Unanswered Questions-A Perspective After 20 Years of Study. *Front Immunol*. 2018;9:1048.

81. Finck R, et al. Normalization of mass cytometry data with bead standards. *Cytometry A*. 2013;83(5):483–494.

82. Zunder ER, et al. Palladium-based mass tag cell barcoding with a doublet-filtering scheme and single-cell deconvolution algorithm. *Nat Protoc*. 2015;10(2):316–333.

83. Zheng Y, Josefowicz S, Chaudhry A, Peng XP, Forbush K, Rudensky AY. Role of conserved non-coding DNA elements in the Foxp3 gene in regulatory T-cell fate. *Nature*. 2010;463(7282):808–812.

84. Povoleri GAM, et al. Human retinoic acid-regulated CD161+ regulatory T cells support wound repair in intestinal mucosa. *Nat Immunol*. 2018;19(12):1403–1414.

85. Picelli S, Björklund ÅK, Faridani OR, Sagasser S, Winberg G, Sandberg R. Smart-seq2 for sensitive full-length transcriptome profiling in single cells. *Nat Methods*. 2013;10(11):1096–1098.

86. Picelli S, Faridani OR, Björklund AK, Winberg G, Sagasser S, Sandberg R. Full-length RNA-seq from single cells using Smart-seq2. *Nat Protoc*. 2014;9(1):171–181.

87. Trombetta JJ, Gennert D, Lu D, Satija R, Shalek AK, Regev A. Preparation of Single-Cell RNA-Seq Libraries for Next Generation Sequencing. *Curr Protoc Mol Biol*. 2014;107:4.22.1–4.2217.

88. Dobin A, et al. STAR: ultrafast universal RNA-seq aligner. *Bioinformatics*. 2013;29(1):15–21.

89. García-Alcalde F, et al. Qualimap: evaluating next-generation sequencing alignment data. *Bioinformatics*. 2012;28(20):2678–2679.

90. Liao Y, Smyth GK, Shi W. featureCounts: an efficient general purpose program for assigning sequence reads to genomic features. *Bioinformatics*. 2014;30(7):923–930.

91. Patro R, Duggal G, Love MI, Irizarry RA, Kingsford C. Salmon provides fast and bias-aware quantification of transcript expression. *Nat Methods*. 2017;14(4):417–419.

92. Love MI, Huber W, Anders S. Moderated estimation of fold change and dispersion for RNA-seq data with DESeq2. *Genome Biol*. 2014;15(12):550.

93. Soneson C, Love MI, Robinson MD. Differential analyses for RNA-seq: transcript-level estimates improve gene-level inferences. *F1000Res*. 2015;4:1521.

94. Mootha VK, et al. PGC-1alpha-responsive genes involved in oxidative phosphorylation are coordinately downregulated in human diabetes. *Nat Genet*. 2003;34(3):267–273.

95. Subramanian A, et al. Gene set enrichment analysis: a knowledge-based approach for interpreting genome-wide expression profiles. *Proc Natl Acad Sci USA*. 2005;102(43):15545–15550.

96. Liberzon A, Birger C, Thorvaldsdóttir H, Ghandi M, Mesirov JP, Tamayo P. The Molecular Signatures Database (MSigDB) hallmark gene set collection. *Cell Syst*. 2015;1(6):417–425.